SHEAR PERFORMANCE OF PRESTRESSED DECKED BULB T BEAMS REINFORCED WITH CFRP STIRRUPS

Nabil F. Grace, PhD, PE, Lawrence Technological University, Southfield, MI
Kenichi Ushijima, North America Cable Technologies, Novi, MI
Soubhagya K. Rout, Lawrence Technological University, Southfield, MI
Mena Bebawy, PhD, Lawrence Technological University, Southfield, MI

ABSTRACT

Carbon fiber reinforced polymer (CFRP) materials have been widely considered as a potential non-corrosive alternative to steel reinforcement in bridge construction. Numerous studies have been carried out to examine the flexural behavior of CFRP prestressed concrete beams. However, the shear behavior of bridge beams with CFRP stirrups has not been thoroughly examined. This paper presents an extensive experimental investigation performed to evaluate the shear behavior of prestressed bridge beams with CFRP stirrups. First, test specimens were prepared according to test standards to evaluate the effect of bend diameter and splice length on the strength of CFRP stirrups. Then, three prestressed decked bulb T beams with a span of 31 ft. (9.45 m) were constructed with longitudinal and transverse CFRP reinforcement. The beams were instrumented and tested to failure under shear loading setup. Half of the span of each beam was reinforced with CFRP stirrups, while the other half was reinforced with steel stirrups. Both ends of each beam were tested under the same shear loading setup. Finally, numerical models for the test beams were developed to validate the experimental findings. Beam ends with CFRP stirrups failed in shear compression due to concrete web crushing while the beam ends with steel stirrups failed in shear tension due to stirrups yielding followed by concrete web crushing. The outcomes of this comprehensive investigation are currently being incorporated in the design and construction documents of M-102 prestressed concrete bridge girders in Southfield, Michigan.

KEYWORDS: Carbon fiber composite cable, Prestressed, Shear, Non-corrosive stirrups, Lap splice, CFRP bend effect.

INTRODUCTION

In order to address corrosion related problems in prestressed concrete (PC) structures, non-corrosive reinforcement materials such as CFRP materials have emerged as an innovative and efficient alternative to conventional steel reinforcement. Extensive research effort has been dedicated to evaluate the flexural behavior of bridge beams prestressed with longitudinal CFRP strands.[1] However, the shear behavior of beams with CFRP stirrups has not been thoroughly investigated. Some researchers evaluated the shear performance of reinforced concrete beams with CFRP as a primary longitudinal reinforcement but most of these studies were conducted without transverse reinforcement.[2,3] Therefore, the use of CFRP stirrups as a shear resisting element has not been really evaluated.

Unlike steel stirrups, where the yield strength and consequently the shear capacity are well determined, the ultimate strength or the shear capacity of CFRP stirrups is influenced by different factors, For instance, CFRP materials are anisotropic in nature. Therefore, bending the CFRP bars/strands to form the required shape of the stirrups involves a significant reduction in the tensile strength at the bend locations, which can lead to premature failure.[4,5]. In addition, to facilitate the construction, bridge beams such as box beams are often constructed by splicing the stirrups to allow a two-stage concrete placement. The splice length of steel stirrups is well developed. However, the splice length of CFRP bars/strands has not been adequately established and consequently, the design strength of the lap splice remains uncertain. ACI-440 committee[6,7] and various other international organizations[8,9,10] provide design guidance for the use of CFRP as internal shear reinforcement. Nevertheless, due to the adoption of different shear resistance methodologies, there are significant discrepancies among available shear design guidelines for beams with CFRP stirrups. The presented experimental/numerical program in this article aims at evaluating the shear performance of prestressed concrete bridge beams provided with CFRP stirrups, and compare this performance with that of beams with steel stirrups.

EXPERIMENTAL PROGRAM

The experimental program was divided into three phases. Phase I evaluated the ultimate tensile strength at the bend locations of CFRP strands/stirrups. CFRP specimens with different bend-radius-to-diameter ratios (R/d) were tested according to standard ACI 440.3R-12 B.5[11] and JSCE-97 E-531[9] test methods. Phase II evaluated the strength of CFRP lap splices embedded in prestressed concrete prisms. The test specimens in this phase were evaluated under a uniaxial tension test setup to determine the failure stress of CFRP lap splice. In order to simulate the effect of concrete confinement due to axial prestressing force, the concrete prisms were compressed between two steel plates bolted together using high-strength bolts. Finally, Phase III of the experimental program addressed the performance and contribution of the CFRP stirrups to the shear carrying capacity of prestressed concrete decked bulb T beams. Three decked bulb T beams were constructed, instrumented, and tested under shear loading setup with varying stirrup spacing. Half of the span of each beam was provided with CFRP stirrups, while the other half was provided with steel stirrups at similar

center-to-center spacing. The ends of each beam were tested subsequently under the same shear loading setup to failure.

PHASE I- CFRP BEND STRAND/STIRRUP SPECIMENS

Several specimens with different bend configurations were tested. The specimens were divided into two groups based on the test method, Group I specimens were tested according to B.5 test method of ACI 440.3R-12 while Group II specimens were tested according to E-531 test method of JSCE-97. Fig. 1 and Table 1 show the configurations and dimensions of the test specimens. Test specimens of Group I were in the form of U-shape with bend portion embedded in concrete blocks as shown in Fig. 2. A tensile force was applied through the straight portion of the strand/stirrup. The specimens were de-bonded on the standard hook end inside the concrete block. Five specimens were tested for each R/d ratio. According to the test standards in ACI 440.3R-12, transverse steel reinforcement was provided at a center-to-center spacing of 3 in. (75 mm) in each of the concrete blocks to prevent splitting of concrete prior to failure of the CFRP bend strand/stirrup specimens. To minimize friction, the blocks were placed on rollers. The two concrete blocks were pushed apart with a uniform loading rate using a hydraulic jack until failure. The distance between the two concrete blocks was adjusted to 20 in. (508 mm).

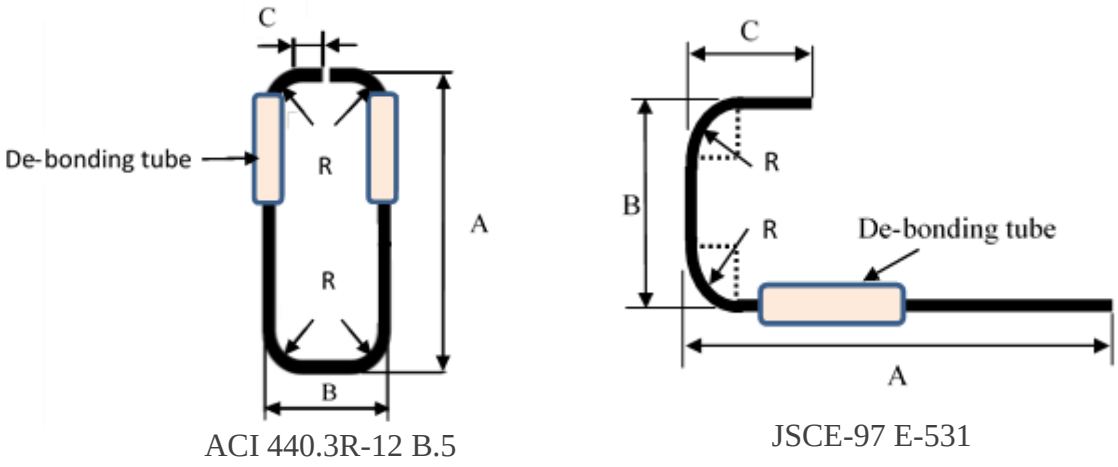

Fig. 1. Details of bend test specimens

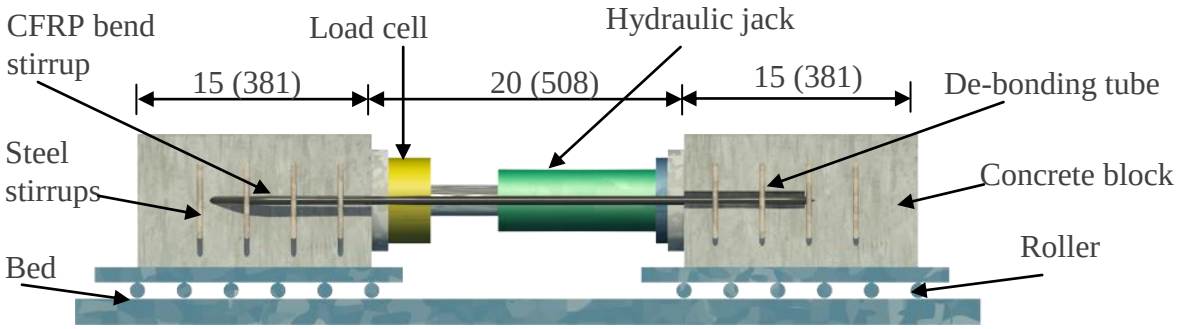

Fig. 2. Details of test specimen according to ACI 440.3R-12 B.5 test method

As shown in Fig. 3, Group II specimens were in form of L-shape with the bend portion embedded inside a concrete block. The straight portion of the CFRP strand/stirrup inside the concrete block was de-bonded using a plastic tube. According to JSCE-97 E-531 test method, the straight leg of the strand was subjected to a uniaxial tensile load using a hydraulic jacking system.

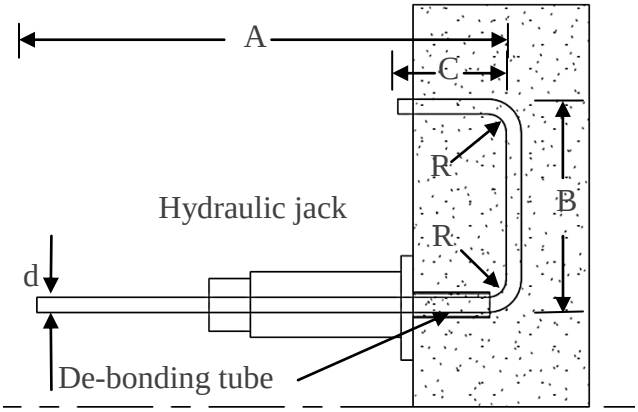

Fig. 3. Details of test specimen according to JSCE-97 E-531 test method

Table 1. Material properties of tested CFRP bend stirrup specimens

	Units	Group-I, ACI 440.3R-12 B.5				Group-II, JSCE-97 E-531		
Bend radius, R	in. (mm)	2.5 (63)	2.5 (63)	6.5 (165)	6.5 (165)	2.0 (51)	1.0 (25)	1.2 (30)
Strand diameter, d	in. (mm)	0.5 (13)	0.6 (15.2)	0.5 (13)	0.6 (15.2)	0.6 (15.2)	0.5 (12.5)	0.6 (15.2)
R/d	----	4.6	3.1	12.7	10.5	3.3	1.9	2.0
A	in. (mm)	38.2 (969)	38.4 (975)	46.2 (1173)	46.4 (1179)	38.0 (965)	36.8 (936)	37.5 (953)
B	in. (mm)	18.2 (461)	18.4 (467)	26.2 (666)	26.4 (671)	15.7 (400)	13.4 (342)	14.1 (359)
C	in. (mm)	6.3 (161)	6.3 (161)	6.3 (161)	6.3 (161)	9.3 (236)	9.3 (236)	9.3 (236)
Average breaking load, F_u	kip (kN)	46.2 (206)	69.0 (307)	46.2 (206)	69.04 (307)	68.4 (304)	46.7 (208)	68.4 (304)
Experimental bend strength, F_{ub},	kip (kN)	38.7 (172)	53.2 (237)	57.7 (256)	72.7 (323)	38.7 (174)	17.8 (80)	33.1 (147)
Experimental reduction factor	----	0.42	0.39	0.62	0.60	0.57	0.38	0.48
ACI 440.4R-04 reduction factor	----	0.34	0.27	0.75	0.63	0.28	0.21	0.21
ACI 440.1R-06 reduction factor	----	0.53	0.46	0.94	0.82	0.47	0.40	0.40
Mode of failure	----	Slippage	Slippage	Slippage	Slippage	Strand rupture	Strand rupture	Strand rupture

The experimental strength reduction factors for the CFRP bend strand/stirrup in both test methods were calculated by dividing the failure load of bend strand/stirrup by the tensile strength of straight strand/stirrup. Further, the test results were compared to the analytical reduction factors provided by ACI 440[6,7] design equations given below,

$$f_{fb} = [0.25 \le (0.05\frac{r_b}{d_b} + 0.11) \le 1.0] \times f_{fu} \le f_{fu} \quad (1)$$

$$f_{fb} = (0.05\frac{r_b}{d_b} + 0.3) f_{fu} \le f_{fu} \quad (2)$$

where,
f_{fb} = design tensile strength of FRP bend stirrup, psi (MPa);
r_b = radius of bend, in. (mm);
d_b = diameter of CFRP strand, in. (mm); and
f_{fu} = design tensile strength of CFRP straight stirrup, psi (MPa).

Test Results

Table 1 and Fig. 4 show the relationship between CFRP bend strength reduction coefficient and R/d ratio compared with the predicted reduction factors according to ACI 440.1R-06 and ACI 440.4R-04. The strength of the CFRP bend strand/stirrup decreased with decreasing the bend radius.. All test specimens in Group I failed due to slippage of the CFRP bonded part (tail length and bend portion) with no rupture of the CFRP strands at the bend portion. Group II specimens failed due to rupture of CFRP strands at the end of the de-bonded length near the bend portion inside the concrete block. The embedment length of the CFRP bend strand in Group I specimens was not long enough to allow failure at the bend. JSCE-97 E-531 test method was more appropriate than ACI 440.3R-12 B.5 test method in evaluating the bend capacity of CFRP strands/stirrups.

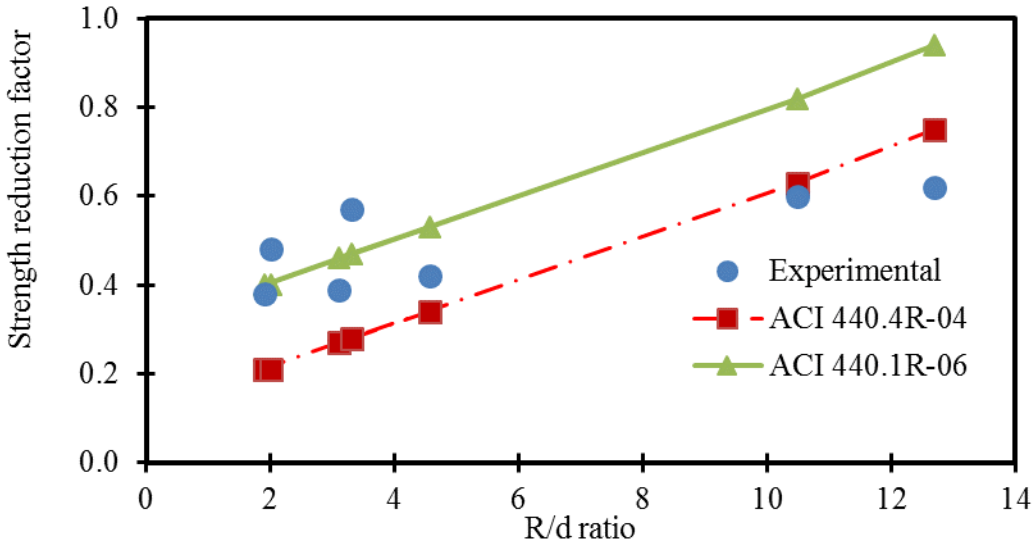

Fig. 4. Strength reduction factor versus R/d ratio

PHASE II- CFRP LAP SPLICE SPECIMENS

To evaluate the strength of CFRP lap splice, three groups of test specimens with lap splice lengths of 15, 20, and 25 in. (381, 508, and 635 mm) were loaded to failure under a uni-axial tensile test setup. Each test specimen consisted of two 0.6-in. (15.2-mm) diameter CFRP strands spliced together inside a concrete prism. The cross-section dimensions of the concrete prisms represented the spacing between the stirrups and the web thickness of the prestressed concrete box beams in M-102 spread box beam bridge in Southfield, MI (currently under construction and expected to be completed by the end of 2013). . The height of the concrete prism represented the CFRP lap splice length. Fig. 5 shows details of the test specimens and the test setup. To simulate the prestressing effect on the CFRP lap splice, two steel plates along the length of concrete prism sandwiched and compressed the specimen using high-strength bolts. The average simulated concrete compressive stress due to bolt tightening was around 1.1 ksi (7.2 MPa).

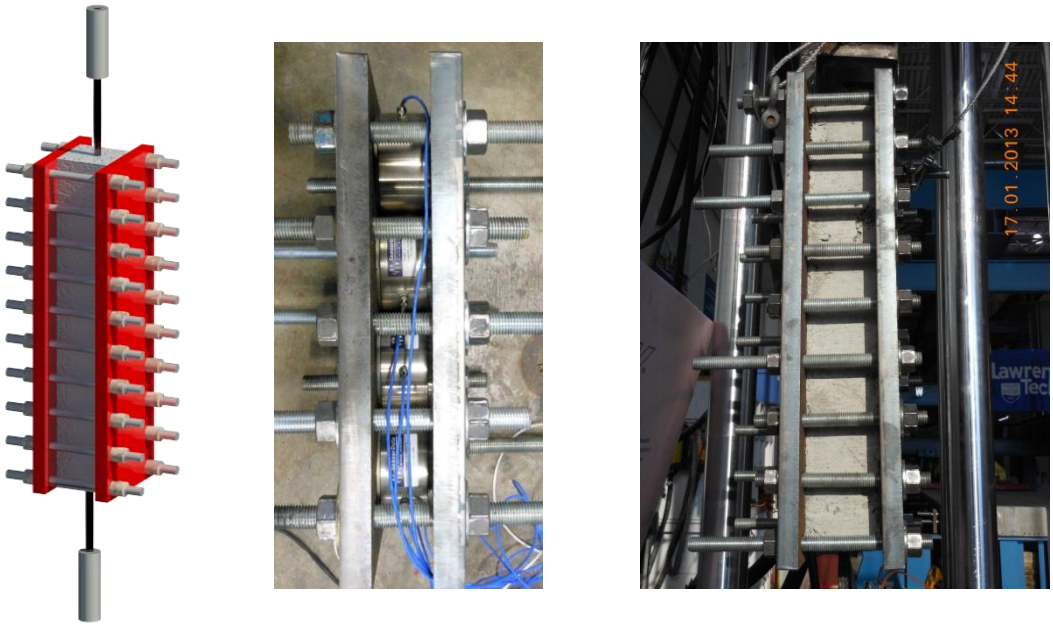

(A) (B) (C)

Fig. 5. (A) Lap splice specimen test setup. (B) Calibration of bolt forces using multiple load cells. (C) Test specimen under uni-axial tension.

Test Results

Table 2 shows a summary for the lap-splice test results. The results in the Table are the average for at least three test specimens. Failure occurred due to slippage of the CFRP strand from the concrete prism. The slippage was associated with the development of a longitudinal crack along the length. For specimens with a web thickness of 4.5 in. (114 mm), the average

failure stresses were 104, 122, and 149 ksi (713, 840, and 1027 MPa) for 15, 20, and 25 in. (381, 508, and 635 mm) CFRP lap splice length, respectively. Similarly, the average failure stresses for specimens with a web thickness of 8 in. (203 mm) were 157, 170, and 231 ksi (1082, 1171, and 1590 MPa), respectively. It can be observed that the failure load increased with the increase in splice length and web thickness. This indicated that the strength of the CFRP lap splice is affected not only by the splice length but also by the surrounding concrete.

Table 2. Summary of CFRP lap splice test specimens

Width of web, in. (mm)	Splice length, in. (mm)	Average stress in CFRP at failure, ksi (MPa)	Ultimate strength of CFRP strands ksi (MPa)	Strength reduction factor (%)
4.5 (114)	15 (381)	103.4 (713)	385 (2646)	26
8.0 (203)	15 (381)	157.0 (1083)		40
4.5 (114)	20 (508)	121.9 (841)		32
8.0 (203)	20 (508)	169.8 (1171)		44
4.5 (114)	25 (635)	149.0 (1028)		39
8.0 (203)	25 (635)	230.6 (1590)		60

PHASE III- PRESTRESSED CONCRETE DECKED BULB T BEAMS

Three prestressed concrete decked bulb T beams were constructed, instrumented and tested to failure under shear loading setup. The beams had an effective span of 31 ft (9.45 m) and cross section dimensions as shown in Fig. 6. Each beam was reinforced with four prestressing and ten non-prestressing seven-wire CFRP strands.[12] All the strands had a diameter of 0.6 in. (15.2 mm) and effective cross sectional area of 0.18 in.^{2} (116 mm^2).

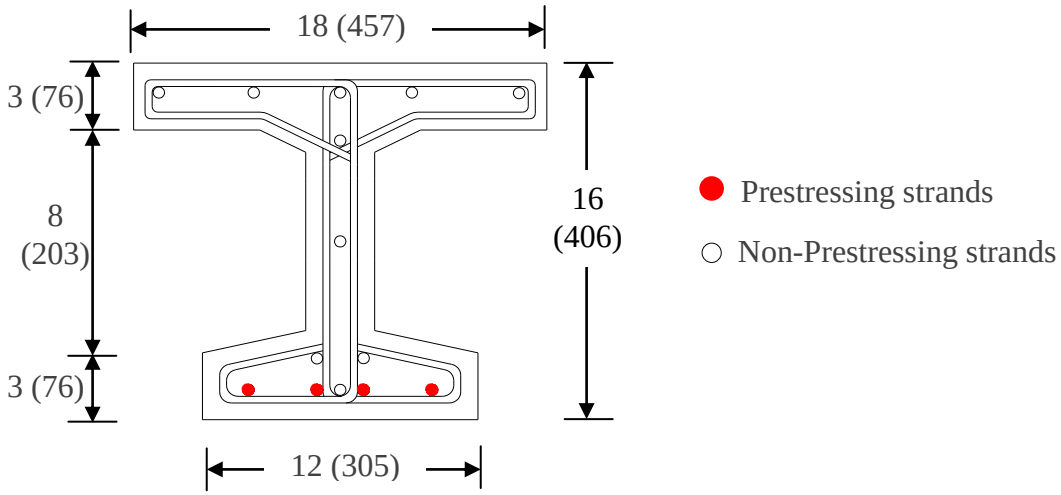

Fig. 6. Cross section of prestressed decked bulb T beam

The prestressing CFRP strands were pretensioned with an initial effective force of 25 kip (111 kN) per strand. Half of the span of each beam was provided with No. 3 (M10) steel stirrups, while the other half was provided with CFRP stirrups with a diameter of 0.41 in. (10.5 mm). Table 3 shows the material properties of the reinforcement. The beams were identical except for the stirrup spacing, which was taken as 4, 6, and 8 in. (102, 152, and 203 mm) in the three test beams. The prestressing system of the CFRP strands was carried out using a newly developed mechanical anchorage system which can be found elsewhere.[1] After pouring the concrete, the beams were covered with wet burlaps and plastic sheets to maintain moisture and were allowed to cure for a period 7 days . The concrete mix achieved an average 28-day compressive strength of 9,000 psi (62 MPa). The concrete compressive strength averaged around 6,400 psi (44.13 MPa) at the time of prestress release.

Table 3. Material properties of reinforcement

Material property	Units	CFRP longitudinal reinforcement	CFRP stirrups	Steel stirrups
Designation		CFRP 1 X 7	CFRP 1 X 7	# 3
Diameter	in. (mm)	0.60 (15.2)	0.41 (10.5)	0.38 (10)
Effective cross- sectional area	$in.^2$ (mm^2)	0.18 (116)	0.09 (58)	0.11 (71)
Linear density	lb/ft (g/m)	0.15 (223)	0.08 (119)	0.38 (565)
Guaranteed breaking load	kip (kN)	60.7 (270)	31.70 (141)	--------
Yield strength	ksi (MPa)	---------	---------	60 (414)
Tensile strength	ksi (MPa)	424 (2,930)	411.91 (2,840)	90 (620)
Elastic modulus	ksi (MPa)	21,610 (149,000)	21,760 (150,030)	29,000 (200,000)
Elongation	%	2.1	1.9	4.9

Instrumentation and Test Setup

Strain gages were attached to the non-prestressing and prestressing CFRP strands near the loading point and to the vertical leg of the CFRP and steel stirrups through the shear span. Strain gages were also attached and to the top flange surface and at the mid-depth of the web. Linear motion transducers (LMTs) were attached to the soffit of the beam to measure deflection during the test. Linear variable differential transducers (LVDTs) were mounted on the web within the critical shear span, in sets of three LVDTs arranged at 0^0, 45^0 and 90^0 directions. The readings were later used to evaluate the shear crack width using a relationship given by Shehata.[13] All different sensors were calibrated and connected to a central digital data acquisition system, which used interface software to record various strain and deflection readings of the beams during the test. The beams were simply supported over a set of

reinforced elastomeric neoprene bearing pads and were loaded with to a concentrated vertical load, applied by an MTS 220 kip (1,000 kN) hydraulic actuator. The shear span of all test beams, the distance from the center of the support to the loading point, was maintained at 45 in. (1143 mm), which corresponded to a shear span-to-depth ratio of 3.0. Fig. 7 shows instrumentation and test setup for the test beams.

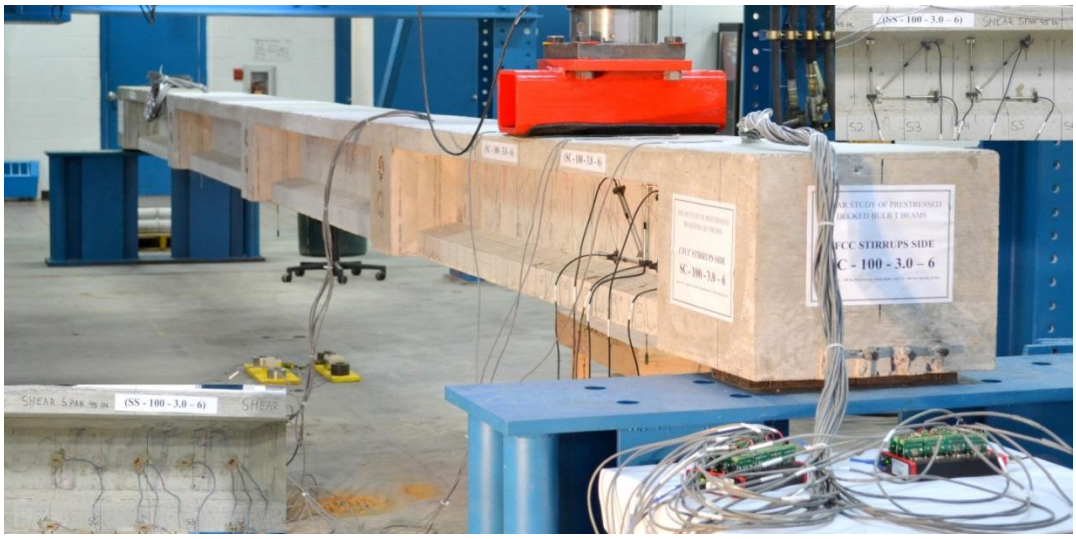

Fig. 7. Shear load setup of prestressed decked bulb T beam

Test Scenario

The testing scenario was performed by first loading beam end with CFRP stirrups to failure and then loading the other beam end with steel stirrups to failure. At either beam end, the load was applied through several loading/unloading cycles with an increment of 2 kip (9 kN) per load cycle. Crack mapping was performed at the end of each load cycle to record the initiation and propagation of cracks. The last load cycle included loading the beam end to failure.

Test Results and Discussion

The results demonstrated a bilinear load-deflection relationship with the formation of cracks marking the loss in stiffness and consequently the change in slope of the relationship. This can be attributed to the shear resistance mechanism. Prior to concrete cracking, the shear force was mainly resisted by the gross un-cracked concrete section. Consequently, the variation of stirrup spacing and stirrup material type (CFRP/steel) did not significantly affect the load-deflection characteristics before cracking. As shown in Table 4, it can be observed that the cracking shear forces of beam ends with either CFRP or steel stirrups were similar. This is because all the beams had a similar longitudinal CFRP reinforcement and a similar level of prestressing force. The letter in the beam notation represents the stirrup material (S for steel and C for CFRP), while the number represent the stirrup spacing in inches.

Table 4. Summary of test results of tested beams

Beam	Cracking Shear Force, kip, (kN)		Ultimate Shear Force, kip, (kN)		Deflection Under Load, in. (mm)		Compressive concrete Strain at the Top, $\mu\varepsilon$		Maximum Stirrup Strain, $\mu\varepsilon$		Mode of Failure
	Exp.	FEA	Exp.	FEA	Exp.	FEA	Exp.	FEA	Exp.	FEA	
C-4	27.8 (124)	28.5 (128)	53.7 (239)	54.5 (242)	1.3 (33)	1.3 (34)	1,042	1,246	3,023	2,058	Web crush
S-4	30.6 (136)	28.5 (128)	68.1 (303)	69.2 (307)	1.7 (43)	1.9 (49)	1,937	1,696	2,538	2,334	Shear tension
C-6	26.8 (119)	28.5 (128)	58.6 (260)	59.8 (266)	1.6 (41)	1.6 (41)	1,282	1,388	3,588	2,885	Web crush
S-6	27.3 (121)	28.5 (128)	61.2 (272)	62.1 (276)	1.4 (36)	1.7 (43)	1,642	1,525	6,429	2,894	Shear tension
C-8	28.1 (124)	28.5 (128)	53.1 (236)	53.7 (239)	1.4 (36)	1.2 (30)	1,531	1,225	3,999	3,233	Web crush
S-8	28.1 (124)	28.5 (128)	51.0 (226)	51.5 (229)	1.2 (31)	1.2 (30)	1,381	1,298	4,869	2,408	Shear tension

After cracking, there was redistribution for the stresses. The applied shear force was resisted by the un-cracked concrete portion, the stirrups intersecting the cracks, and through the aggregate interlock through the crack. There was a significant change in the strain of stirrups around cracking shear force, which indicated the active participation of the stirrups in the shear resistance mechanism. The number of stirrups involved in the shear resistance varied with the change in stirrup spacing.

As shown in Fig. 8, the common mode of failure in beam ends with CFRP stirrups was concrete web crushing (shear compression), while yielding of stirrups (shear tension) followed by concrete web crushing was the common failure mode in beam ends with steel stirrups. The difference in the mode of failure is directly related to the difference in performance between CFRP and steel materials. With higher load levels, steel stirrups exhibited a yield plateau, which was characterized by a significant increase in strain with a little increase in the load carrying capacity. This excessive increase in the strain allowed shear cracks to propagate and open widely, which reduced the shear carrying capacity through the aggregate interlock and resulted in failure. On the other hand, CFCC stirrups did not exhibit any yield plateau and therefore, the strain of the stirrups increased linearly with increasing the shear load until the shear crack became excessive and wide enough to reduce the shear aggregate interlock and stress the concrete to failure. Fig. 9 shows the relationship between the shear force and stirrup strain of the test beams. There was no rupture of the CFRP stirrups but it was noticed that the maximum strain attained in the CFRP stirrups increased with increasing the stirrup spacing. Overall, the maximum strain attained in the CFRP stirrups at the ultimate shear force was much higher than the current 2,000 με design

strain limit specified by ACI 440.4R-04 shear design guidelines, while ACI 440.1R-06 design strain limit of 4,000 με seems reasonable as a defining level for shear failure. The steel stirrups, on the other hand, experienced yielding. The yielding shear force decreased with increasing the stirrup spacing.

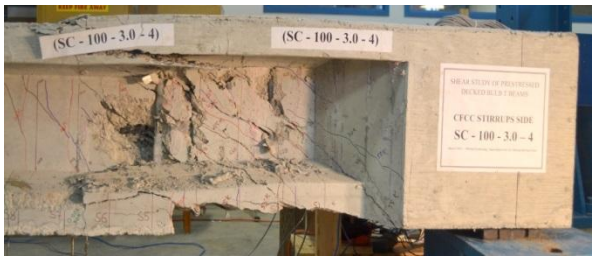

Beam end C-4 (Web crushing)

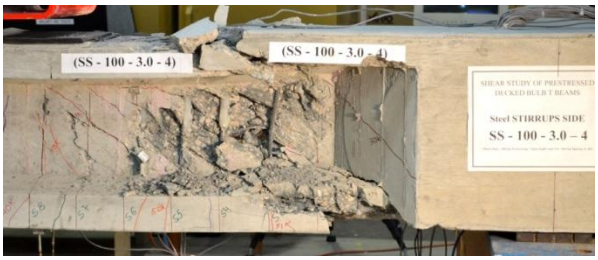

Beam end S-4 (Yield of stirrups)

Beam end C-6 (Web crushing)

Beam end S-6 (Yield of stirrups)

Beam end C-8 (Web crushing)

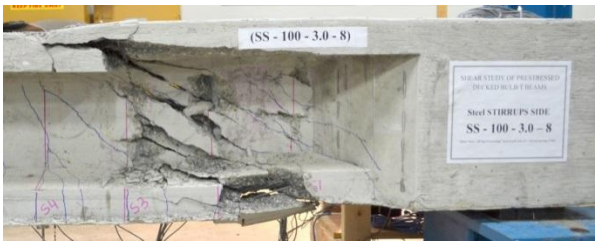

Beam end S-8 (Yield of stirrups)

Fig. 8. Failure of test beams

Deflection under the loading point is presented in Table 4 and Fig. 10. All of the test beams failed in shear with no rupture or de-bonding of the longitudinal CFRP prestressing strands. The concrete compressive strain (Fig. 11) for the test beams was recorded at the top concrete surface near the loading point. The maximum strain attained at ultimate shear force ranged from -1,042 to -1,531 με for beam ends with CFRP stirrups while it ranged from -1,381 to -1,937 με for beam ends with steel stirrups. The shear force versus concrete strain relationship also exhibited a bilinear relationship with an apparent change in slope near the cracking shear force. Linear Variable Differential Transducers (LVDTs) were used to measure the shear crack width using the crack width relationship.[13] It was noticed that at any particular shear force level, the crack width increased with increasing the stirrup spacing and it was higher for beam ends with CFRP stirrups compared to that for ends with steel stirrups (Fig. 12). With increasing the stirrup spacing, the number of cracks within the critical shear span decreased but the width of the each individual crack increased. In other words, increasing the stirrup spacing resulted in fewer but wider cracks.

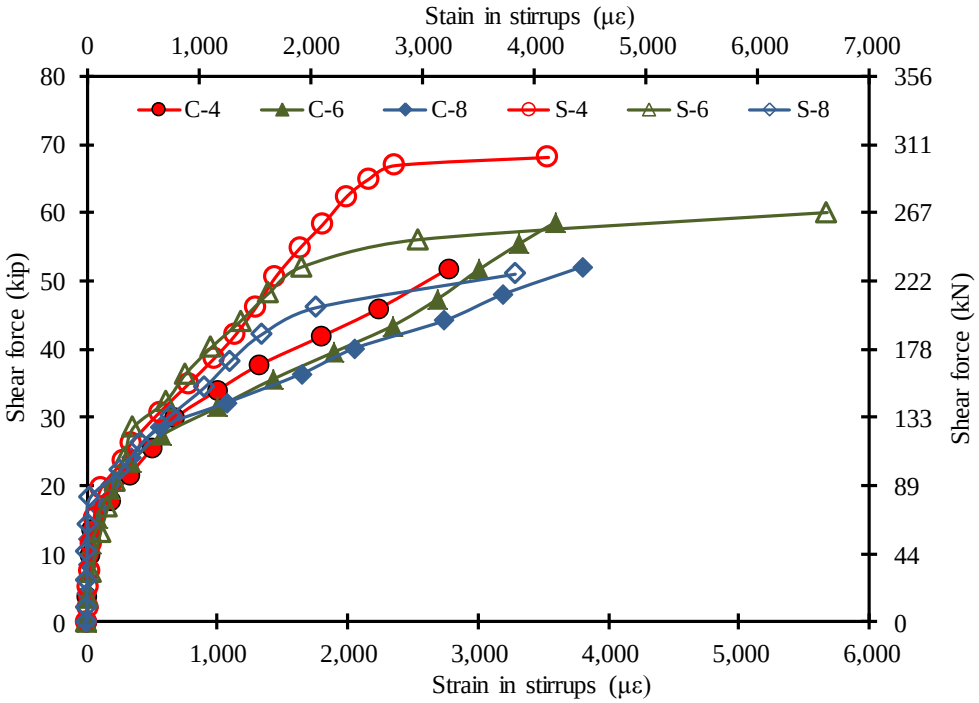

Fig. 9. Shear force versus strain in stirrups curves in test beams

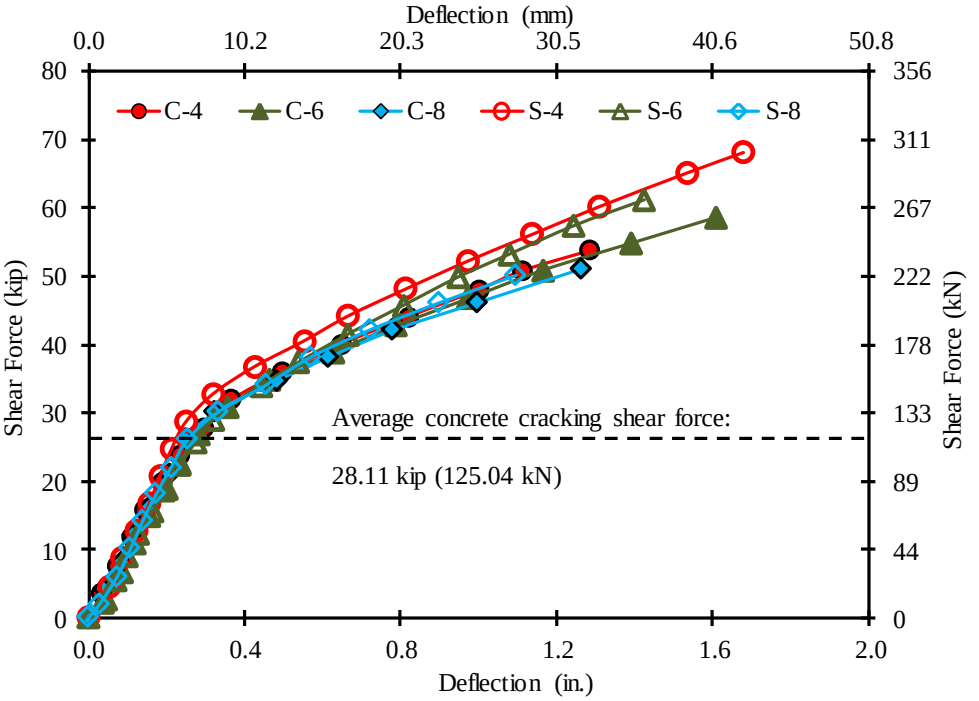

Fig. 10. Shear force versus under-load deflection for all test specimens

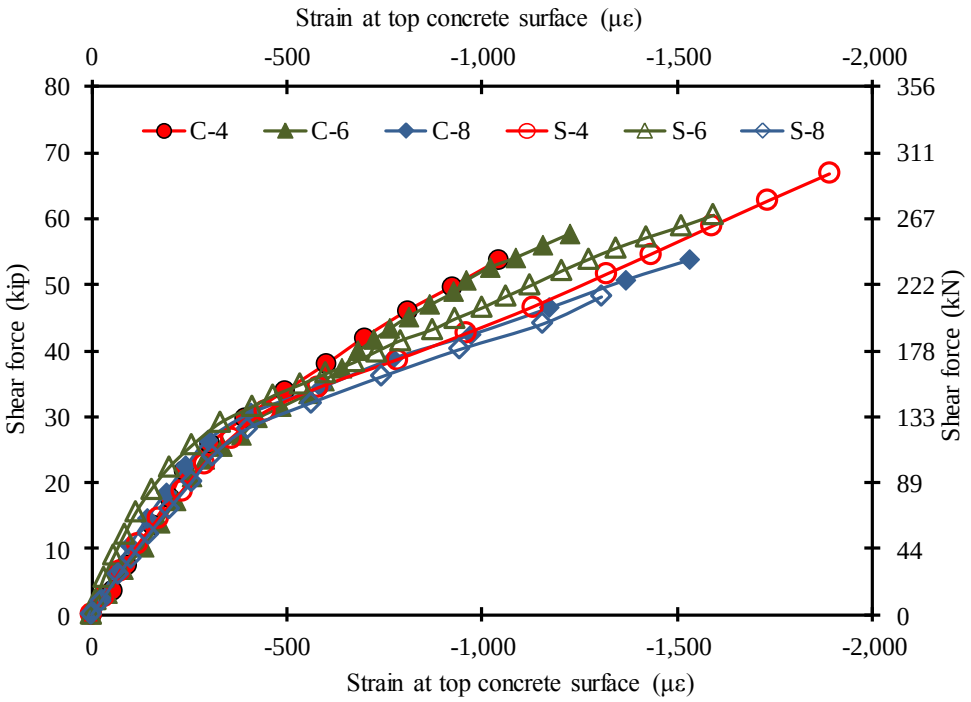

Fig. 11. Concrete strain versus shear force relationship for test beams

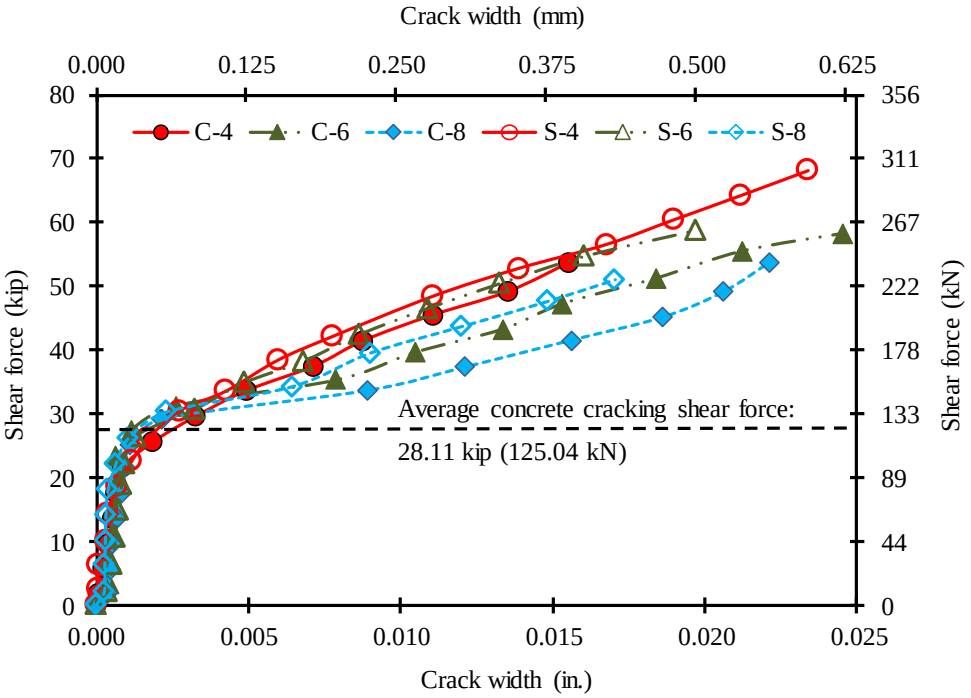

Fig. 12. Average crack width for test beams

NUMERICAL ANALYSIS

Finite element models for the experimental beams were generated using a commercially available software.[14] The beams were modeled using a three-dimensional eight-node linear brick element C3D8R. A continuum plasticity based concrete damage model was used in modeling the concrete material. The model combines plasticity with isotropic strain hardening followed by isotropic or anisotropic concrete damage. Concrete material was defined with Young's modulus of 4.91×10^3 ksi (34 GPa) and Poisson's ratio of 0.2 in addition to concrete compressive and tensile stress-strain curves. The internal reinforcement of the beams including the longitudinal and transverse reinforcement was modeled using a two-node linear 3D truss element (T3D2) with three degrees of freedom at each node. Fine details of the finite element models can be found elsewhere.[1] The response of the numerical models were compared to that of the experimental beams as shown in Table 4 and Fig. 13. The deflection and strain responses of the generated FEA models matched closely those obtained experimentally. The FEA models predicted the failure mode and region agreeably with the experimental beams. Overall, it can be concluded that FE models accurately simulated the shear performance of the test beams.

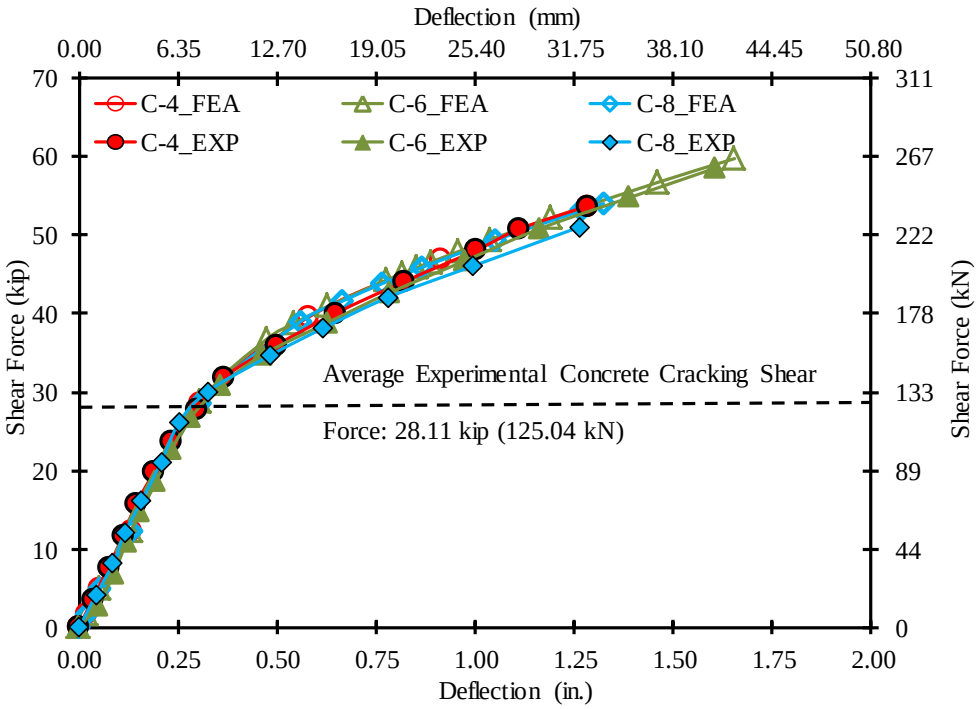

Fig. 13. Shear force versus under-load deflection curves (experimental vs. numerical)

The obtained experimental/numerical results were compared with the analytical prediction from various national and international shear design guidelines such as, ACI 440.1R-06 and ACI 440.4R-04 in the U.S.A., CSA S806-12 and ISIS M3-07 in Canada, and JSCE-97 in

Japan. The comparison between experimental shear strength (V_{exp}) and predicted shear strength (V_{pred}) using different design guidelines is shown in Fig. 14. ACI 440.4R-04 shear design equations for prestressed concrete structures showed a conservative nominal shear resistance with an average experimental-to-predicted ratio of 2.0. CSA S806-12 predicted the nominal shear resistance with an average experimental-to-predicted ratio of 1.0. However, proper modifications are required in the shear design equations given by CSA S806-12 to include the effect of prestressing force in CFRP prestressed concrete structures.

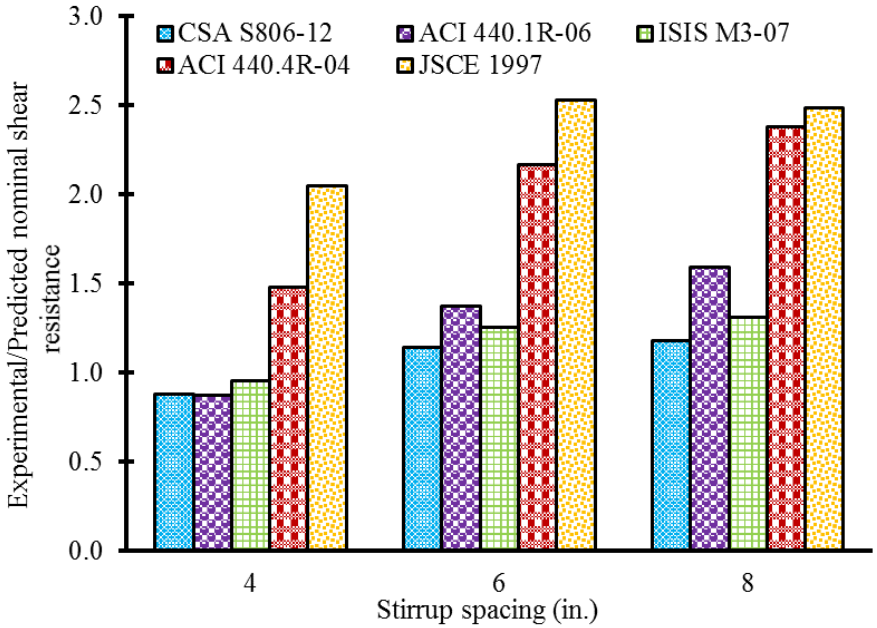

Fig. 14. Ratio between experimental and predicted shear load carrying capacity according to various shear design guidelines.

CONCLUSIONS

The experimental investigation was carried out using on type of CFRP reinforcement with different cross sectional areas. Other types of CFRP reinforcement have not been investigated. Besides, the scale effect was not evaluated through the study and therefore, the results of the investigation may not be directly implemented in the field without proper verification. Based on the results from the experimental/numerical investigation, the following conclusions are made:

1. CFRP strands/stirrups tested according to JSCE-97 E-531 failed at the bend portion while the CFRP strands/stirrups tested according to ACI 440.3R-12 failed due to slippage as the embedment length was not sufficient. The minimum embedment length requirement as per ACI 440.3R-12 B.5 test method needs a revision to permit the failure of the bend portion and eliminate the slippage. Overall, the tensile strength of the CFRP stirrups at the bend location increased with the increasing the bend radius.

2. The failure load of the CFRP lap splice increased with increasing the splice length and web thickness. The average CFRP stress values in specimens with web thickness of 4.5 in. (114 mm) were 103, 122, and 149 ksi (713, 841, and 1028 MPa) for CFRP lap splice lengths of 15, 20, and 25 in. (381, 508, and 635 mm), respectively. Whereas for specimens with 8 in. (203 mm) web thickness the average CFRP failure stress values were 157, 170, and 231 ksi (1083, 1171, and 1590 MPa), respectively.
3. Beam ends with the CFRP stirrups failed in shear compression mode due to concrete web crushing while beam ends with the steel stirrups failed in shear tension mode due to yielding of stirrups followed by concrete crushing in the web. Both modes of failure were quite sudden in nature. Overall, it was noticed that the cracking and ultimate loads of beam ends with CFRP stirrups were close to those of ends with steel stirrups. There was no significant difference in the load-deflection curves either. Therefore, it can be concluded that the performance of beams with CFRP stirrups is similar to the performance of beams with steel stirrups. Nevertheless, CFRP material has the advantage of corrosion resistance, which gives it superiority over steel in region with extreme weather conditions.
4. The maximum strain in the CFRP stirrups increased with increasing the stirrup spacing. The maximum strain in the stirrups at ultimate shear force were 3,023, 3,588 and 3,999 με for stirrup spacing of 4, 6, and 8 in. (102, 152, and 203 mm), respectively. The strain in the stirrups was proportional to the spacing of the stirrups.
5. Because of the lower modulus of elasticity of CFRP compared to steel, beam ends with CFRP stirrups exhibited slightly wider cracks than those observed in ends with steel stirrups. Further, the crack width increased with increasing the stirrup spacing.
6. JSCE-97 and ACI 440.4R-04 conservatively predicted the nominal shear strength with an average experimental-to-predicted ratio of 2.0, whereas CSA S806-12 and ISIS M3-07 predicted the nominal shear strength with an average experimental-to-predicted ratio of 1.0. These shear design equations need revision to eliminate the difference and to include all affecting factors such as the prestressing effect.
7. The numerical models of the test beams accurately predicted the response of the experimental beams. The average differences in the numerical and experimental cracking and ultimate shear forces were around 5 and 2%, respectively.

ACKNOWLEDGEMENTS

This investigation was sponsored through a consortium of: National Science Foundation, U.S.A. (Award No. CMMI-0969676), Federal Highway Administration Transportation Pool Fund (Michigan-DOT, Iowa-DOT, Wisconsin-DOT, Oregon-DOT and Minnesota-DOT) (Award No. TPF-5/254), and Tokyo Rope MFG. Co. LTD, Japan. The authors gratefully acknowledge their supports.

References

1. Grace, N. F., Enomoto, T., Baah, P., and Bebawy, M., "Flexural Behavior of CFRP Precast Prestressed Decked Bulb T-Beams," *Journal of Composites for Construction, ASCE*, V.16, No. 3, 2012, pp. 225-234.
2. Razaqpur, A. G., Isgor, O. B., Greenaway, S., and Selley, A., "Concrete Contribution to the Shear Resistance of FRP Reinforced Concrete Members." *Journal of Composites for Construction, ASCE*, V. 8, No. 5, 2004, pp. 452-460,
3. Tureyen, A. K., and Frosch, R. J., "Shear Tests of FRP Reinforced Concrete Beams without Stirrups," *ACI Structural Journal*, V. 99, No. 4, 2002, pp. 427-434.
4. Maruyama, T., Honama, M., and Okmura, H., "Experimental Study on Tensile Strength of Bend Portion of FRP Rods," *ACI special publications*: Fiber reinforced plastic reinforcement for concrete structures, SP-138, A. Nanni and C. W. Dolan, eds., American Concrete Institute, Farmington Hills, Michigan, 1993, pp. 163-176.
5. Shehata, E., Morphy, R., and Rizkalla, S. H., "Fiber Reinforced Polymer Shear Reinforcement for Concrete Members: Behavior and Design Guidelines," *Canadian Journal of Civil Engineering*, V. 27, No. 5, 2000, pp. 859-872.
6. ACI Committee 440, "Guide for the Design and Construction of Structural Concrete Reinforced with FRP Bars," *ACI 440.1R-06*, American Concrete Institute, Farmington Hills, Mich. 2006, 44p
7. ACI Committee 440, "Prestressing Concrete Structures with FRP Tendons," *ACI 440.4R-04*, American Concrete Institute, Farmington Hills, Mich. 2004, 35p.
8. Canadian Standards Association (CSA), "Design and Construction of Building Components with Fiber-Reinforced Polymers*," CSA Standard CAN/CSA S806-12*, Rexdale, Ontario, Canada, 2012, 206p.
9. Japan Society of Civil Engineers (JSCE), "Recommendations for Design and Construction of Concrete Structures Using Continuous Fiber Reinforced Materials," Research Committee on Continuous Fiber Reinforced Materials, Tokyo, Japan, 1997, 325p.
10. Intelligent Sensing for Innovative Structures (ISIS), "Reinforcing Concrete Structures with Fiber Reinforced Polymers," *ISIS-M03-07*, Canadian Network of Centers of Excellence, Univ. of Winnipeg, Winnipeg, Canada, 2007, 151p.
11. ACI Committee 440, "Guide Test Methods for Fiber Reinforced Polymers (FRPs) for Reinforcing or Strengthening Concrete Structures," *ACI 440.3R-12*, American Concrete Institute, Farmington Hills, Mich. 2012, 27p
12. Tokyo Rope. "CFCC Quality Report," Tokyo Rope Mfg. Co. Ltd., Japan, 2007, 187p.
13. Shehata, E. F. G., "Fibre Reinforced Polymer (FRP) for Shear Reinforcement in Concrete Structures," Ph.D. Dissertation, Department of Civil and Geological Engineering, University of Manitoba, March 1999, 316p.
14. ABAQUS 6.9 User's Manual, Simulia Inc., Providence RI, U.S.A., 2008.